# COST EFFECTIVE BALLISTIC PROTECTION FOR VEHICLES

John D. Jones[1,*], J. David Reinecke[2] and Lwazi Pambuka[1]
[1]School of Mechanical, Industrial and Aeronautical Engineering, University of the Witwatersrand, South West Engineering Building, East Campus, Braamfontein, Johannesburg
john.jones@wits.ac.za
[2]Landward Sciences Impact Area, Defence and Security Cluster, CSIR
Building 45. CSIR Campus, Meiring Naude Drive, Brummeria
DReinecke@csir.co.za

**Abstract**
In the design of protected vehicles there is a constant trade-off between mobility, protection, and cost. To protect against increasing threat levels, designers are usually required to use armour materials with increased mass and thickness. However, this has a negative effect on the vehicle's mobility. Reducing the mass of armour plates for the same level of protection usually requires the use of more expensive materials, thus increasing the cost. The aim of this project was to investigate how the areal density of armour plates, used for vehicle protection against a NATO Level 3 ballistic threat, can be reduced whilst still maintaining the required level of threat protection, and optimising cost by exploring varying material layers in a composite armour plate assembly. This work used computational modelling to evaluate protection capabilities of various combinations of lower cost materials that were then manufactured and tested. The test plate combination initially selected were based on the published computational work of Rahman et al., [2]. These proposed, multilayered, plates computationally provided a reduction in aerial density of 12% compared to equivalent homogeneous amour steel plate. Additional plate combinations, using Strenx 700E Al-7075-T6 with Kevlar and Dyneema layers, were proposed and computationally evaluated and assessed. These multilayered plates were then manufactured and subjected to ballistic tests against NATO level 3 (7.62 x 51 mm Tungsten Carbide (WC)) armour piecing rounds. None of the proposed and computationally verified plates provided the required ballistic protection. The main reason for this is ascribed to the application and use of only published material parameters and the implementation of the failure model.

**Keywords:** Ballistic limit, 7.62 mm bullets, Johnson-Cook, Recht-Ipson

## 1. Introduction

In recent times, there has been an increased interest in using multilayered plates for the protection of structures from ballistic and explosive threats [1–12]. The advantages of using multilayered plates are that the protection can be optimised to utilise the strengths of the different materials to prevent perforation, damage, and shock, whilst potentially reducing the density and mass of the overall plate. There may also be significant benefits in the manufacture and repair [11] of multilayered plates as opposed to their monolithic counterparts, especially as the monolithic thick armour plates are not always manufactured to the specified nominal dimensions [3,8]. There is also a continual drive to reduce the cost of protection provided by armour plates as high quality, monolithic armour plate is significantly more expensive than structural steels. This has specific relevance in the design of protected vehicles where there is a constant competing trade-off between mobility, protection, and cost.

Several researchers have investigated the performance of single monolithic plates versus layered plates. However, the literature shows that there is still some debate as to whether a layered plate configuration can offer equal, or better, protection to an equivalent thickness monolithic plate, noting that this would be comparing the plates performance based on a specific monolithic plate thickness to provide protection against a specific threat level as detailed in [13,14].

Dey *et al.*, [6] investigated the ballistic performance of single and double layer Weldox 700E plates impacted by blunt and ogival projectiles at sub ordnance velocities. Their findings showed that for a total target thickness of 12 mm, the double layer target plate performed better than the single layer monolithic target plate when impacted with a blunt projectile. However, for an ogival projectile, the performance of the layered plates was slightly worse than its monolithic counterpart. This research highlighted that the type of projectile can affect the protection level offered by a specific target plate(s) as well as the fact that the failure mechanism can change, depending on the target plate configuration. These findings have been numerically verified for double layered plates of the same metal in [11] as well as for layered plates of different materials in [9].

In stark contradiction, Wei *et al*. [5] showed that the ballistic performance of a monolithic plate target was better than its layered counterpart when impacted with a blunt projectile which is consistent with the findings in [7,10] for sub-ordinance velocities. As such, there is still a question as to whether using layered plates, of the same or differing material types, offers any benefit in terms of ballistic performance compared to an equivalent thickness monolithic plate, particularly for impact velocities above 500 m/s. It is evident, however, that using layered plates, and the order in which the plates are layered, can affect the failure mechanism of the plates [5,9] and the ballistic performance.

As such, layered armour plates, specifically using different materials, are currently an interesting area of research as they can offer significant weight and / or cost savings. Rahman *et al.* [2] numerically investigated the penetration resistance of different plate configurations against a 7.62 APM2 round at various velocities, to determine whether any of the plate configurations could meet the ballistic limit of 930 ± 20 m/s specified in [13,14] for a level 3 threat, whilst reducing the overall areal density of the plate configurations, when compared to a monolithic armoured plate of 25 mm thickness. The authors investigated using high strength steel and Al7075 T6 layered plate configurations to stop the specified projectile. These computational results by Rahman *et al.* [2] showed that the areal density could be reduced by 20% and still meet the ballistic limit requirements, with triple layered plate configurations performing better than the equivalent areal density double-layered plates.

The work reported in this paper aimed to build on the computational work of Rahman *et al.* [2] and determine whether double and triple layered plates, constructed from lower cost and lower density materials, can be used to meet the NATO Level 3 requirements [13,14] for both a 7.62 APM2 and 7.62 x 51 mm APWC bullet. Both experimental and computational analysis have been used, with the computational models based solely on material data available in published literature. The experimental method applied was to validate the computational threat penetration model, design and test selected plate combinations based on computational results and additional post-test computational modelling with the WC ballistic threat.

## 2. Validation of Numerical Modelling

To validate the ballistic model of a 7.62 APM2 round impacting a target plate, literature data [3,4,12] was used to simulate a 7.62 APM2 round impacting a monolithic 12 mm Weldox 700E target and a monolithic 20 mm Al7075 T651 target, at various velocities, however bullet rotational velocity was not considered following literature [3,4,12].

A finite element model (FEM) of the 7.62 APM2 projectile was created using quarter symmetry in Ansys Explicit Dynamics, as shown in Figure 1, with a mesh size of 0.4 mm being used for both the projectile and the region of interest on the target plates. As far as possible, only 8 node hexahedral elements were used for the meshing. The mesh size was determined by running convergence studies on both the plate and the projectile.

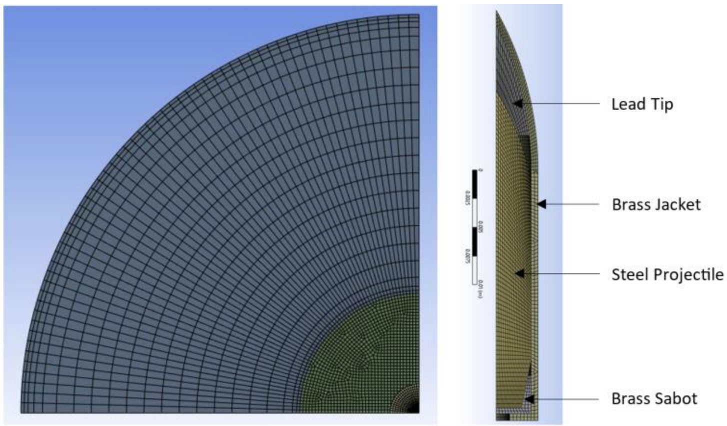


**Figure 1: Quarter symmetry model of 7.62 APM2 bullet and target plate.**

The Johnson-Cook (JC) constitutive model [15] presented in Equation (1) was used to model the material behaviour of both the bullet and the target plates.

$$\boldsymbol{\sigma = [A + B\varepsilon^n][1 + Cln\dot{\varepsilon}^*][1 - T^{*m}]} \tag{1}$$

In Equation (1), $\sigma$ is the von Mises flow stress, $A$ is the yield stress, $B$ and $n$ represent the effects of strain hardening, $\varepsilon$ is the equivalent plastic strain, $\dot{\varepsilon}^*$ is the dimensionless plastic strain at a specific strain rate $\dot{\varepsilon_0}$, $T^*$ is homologous temperature and $C$, $m$ are material constants. The material properties used in the validation models are shown in Table A1, Appendix A.

For the target plates, the JC failure model [16] in Equation (2) was used to model the material failure of both the bullet and the target plates.

$$\boldsymbol{\varepsilon^f = \left[D_1 + D_2 e^{(D_3\sigma^*)}\right][1 + D_4 ln\dot{\varepsilon}^*][1 + D_5 T^*]} \tag{2}$$

In Equation (2), $\varepsilon^f$ is the fracture strain, $D_1$ - $D_5$ are material constants and $\sigma^*$ is the dimensionless pressure-stress ratio. The material constants used for the failure model are shown in Table A2, Appendix A. The material and failure parameters used for the Weldox 700E plate were taken from [12,17] whereas the properties for Al7075 T651 were taken from [18] as the JC failure parameters were not available in the original papers [3,4,12] as a different failure criterion was used.

In ballistic testing and simulation, the ballistic limit ($v_{bl}$) is important as it gives an indication of the maximum velocity that a protective plate can stop for a specified bullet type. A common way of predicting the $v_{bl}$, based on experimental work, is using the Recht-Ipson model [19] in Equation (3).

$$\boldsymbol{V_r = a(V_i^P - V_{bl}^P)^{\frac{1}{P}}} \qquad \textbf{(3)}$$

In Equation (3), $V_r$ is the residual velocity, a is constant which is set to 1 when no plugging occurs during penetration, $V_i$ is the impact velocity and $P$is a fitting constant.

Using in Equation (3) for determining the $v_{bl}$, simulations were run by impacting both the 12 mm Weldox 700E plate and the 20 mm Al7075 T651 plate with a 7.62 APM2 bullet at increasing velocities until the $v_{bl}$ could be determined. These results were then compared to the experimental and Recht-Ipson values from literature [3,4,12], and presented in Figure 2. For the Weldox 700E target plate results shown in Figure 2A, the difference in predicted and experimental $v_{bl}$ value was 2.1%. Note also the small difference between the $P$ value for the Recht-Ipson fits to the experimental data from literature [3] and the simulation. The Aluminium 7075 T651 target plate results in Figure 2B show a larger disparity with a predicted $v_{bl}$ 8.3% higher than the $v_{bl}$ determined using the experimental data from [4]. This disparity is also reflected in the $P$ values. Given that previous results showed an overestimation of 4% for the 12 mm Weldox 700E Plate and 11% for the 20 mm Al 7075 T651 plate [3], these results were considered acceptable validation of the combined bullet and target model.

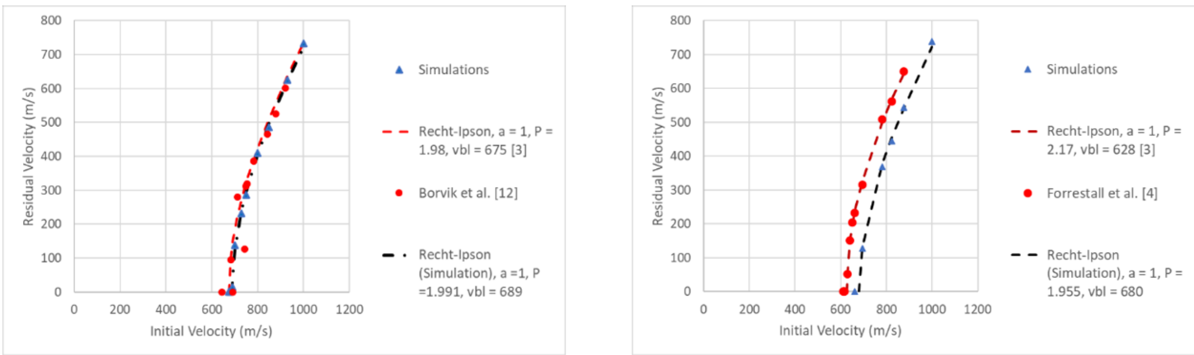


A B

**Figure 2: Comparison of experimental results [3,4,12] and simulation results for a 7.62 APM2 projectile impacting (A) a 12 mm Weldox 700E plate and (B) a 20 mm Al 7075 T651 plate.**

## 3. Design of Target Plates

Using the results of the work in [2] and the authors validated 7.62 APM2 and plate models, the eight different panel configurations shown in Table  were simulated at an impact velocity of 930 m/s from a 7.62 APM2 bullet. The protection plates comprised a combination of lower cost armoured steel Strenx 700F, Aluminium Al7075 T6 and Dyneema® resin matrix panels. The predicted potential reduction in areal density is shown in Table  and is based on the specified areal density of 196.5 kg/m$^2$ for a 25 mm monolithic plates specified in [2]. These plate configurations offered significant weight and cost savings as lower cost steel and less dense materials were chosen. For these targets, the material properties and the failure constants used in the simulations were taken from literature, as experimental data was not available at the time of writing, and are shown in Table A2 and Table A3 noting that the aluminium material and related failure model parameters differed from the validation model.

The image results of these simulations for all combinations listed in Table  showing the final position of the projectile are shown in Figure 3. Only plate combinations B4 and C1 did not stop the bullet at 930 m/s, and full penetration occurred. For plate combination A2, A3 and B3, partial penetration occurred but the bullet was still effectively stopped. Based on these results, and despite the predicted perforations it was decided to physically manufacture and test all these panel configurations.

**Table 1: Description of target plates showing the predicted reduction in areal density for each plate configuration.**

| Code | Description | Layers | Bonded | Areal density ($kg/m^2$) | Reduction in areal density |
|---|---|---|---|---|---|
| A1 | 16 mm Strenx 700E-10 mm Al7075 T6 | 2 | No | 145.14 | 26.1% |
| A2 | 8 mm Strenx 700E-10 mm Al7075 T6-8 mm Strenx 700E | 3 | No | 146.44 | 25.5% |
| A3 | 8 mm Strenx 700E-10 mm Al7075 T6-8 mm Strenx 700E | 3 | Yes | 146.44 | 25.5% |
| B1 | 16 mm Strenx 700E-9 mm Dyneema | 2 | Yes | 134.40 | 31.6% |
| B2 | 8 mm Strenx 700E-9 mm Dyneema-8 mm Strenx 700E | 3 | Yes | 134.40 | 31.6% |
| B3 | 16 mm Strenx 700E-9 mm Aramid | 2 | Yes | 136.67 | 30.4% |
| B4 | 8 mm Strenx 700E-9 mm Aramid-8 mm Strenx 700E | 3 | Yes | 136.67 | 30.4% |
| C1 | 8 mm S355JR-10 mm Al7075 T6-8mm S355JR | 3 | No | 150.90 | 23.2% |

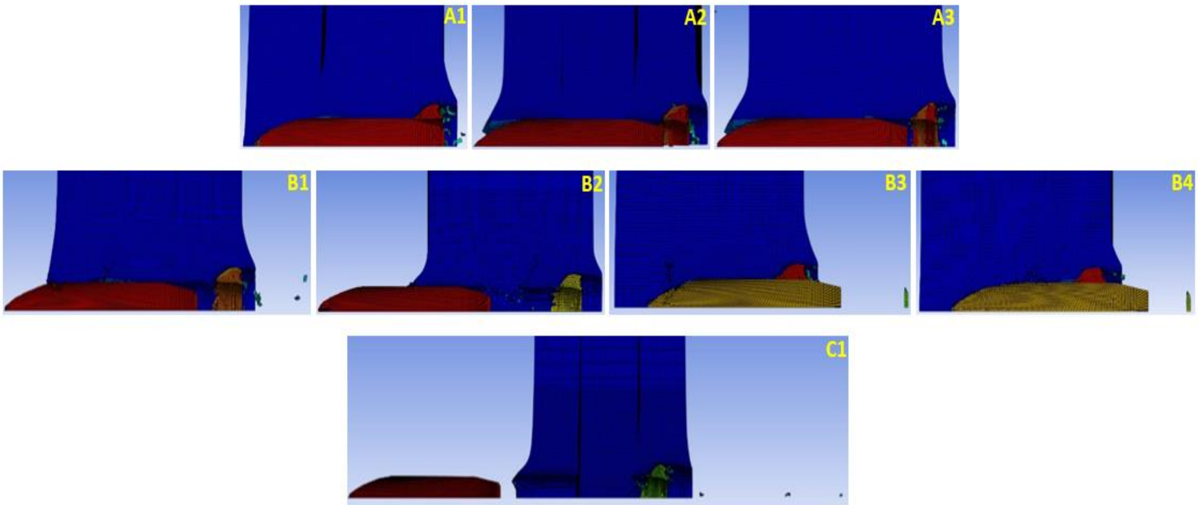


**Figure 3: Images of simulations of designed target plates, Table , versus 7.62 APM2 bullet showing if the bullet was stopped (A1, B3) at 930 m/s or if the plates were partially penetrated (A2, A3, B1) or fully penetrated (B2, C4).**

## 4. Ballistic Testing

All the plate configurations shown in Table  were manufactured and then tested by ARMSCOR. During testing, only the 7.62 x 51 mm Armour Piercing Tungsten Carbide (APWC) bullet was available, and only one velocity was used, namely 930 ± 20 m/s. The target plates were manufactured to dimensions of 300 mm x 300 mm and a maximum of 3 shots were allowed per target plate. The target plates were placed in a frame, 30 m from the barrel. During testing, the $V_i$ and $V_r$ were determined by using Tema Pro T2023a-64 software to analyse the test videos recorded using a Photron SA4 high-speed camera. The average results of the ballistics tests carried out are shown in Table .

As shown in Table , at a nominal impact velocity of 930 ± 20 m/s not one of the panel configurations was able to stop the 7.62 x 51 mm APWC round. Interestingly, for target plates A1, A2 and A3, the ballistic performance of the triple layered plates was better than that of the double layered plate, with the bonded triple layered plate having the lowest average residual velocity value. In contrast, when composite materials were used instead of the Al7075 T6, the double layered plates performed better than the triple layered plates.

**Table 2: Average results of ballistic testing.**

| Target Plate | Average Impact Velocity (m/s) | Average Residual Velocity (m/s) | Number of Shots |
|---|---|---|---|
| A1 | 912.9 | 461.0 | 6 |
| A2 | 928.4 | 452.1 | 6 |
| A3 | 915.3 | 428.8 | 3 |
| B1 | 917.9 | 565.6 | 3 |
| B2 | 915.7 | 596.0 | 3 |
| B3 | 929.5 | 585.1 | 3 |
| B4 | 923.0 | 635.0 | 3 |
| C1 | 917.0 | 493.0 | 3 |

Inspection of the plates post-impact revealed that the Al7075 T6 material exhibited a significantly different failure behaviour when sandwiched between two Strenx 700E (A2, A3) plates to being placed at the unsupported rear layer of the target plate (A1). The exit material failure appears brittle on target plate A1 as opposed to the more ductile failure features evident on the sandwiched A2 and A3 configurations. These exit hole material failures are shown in Figure 4.

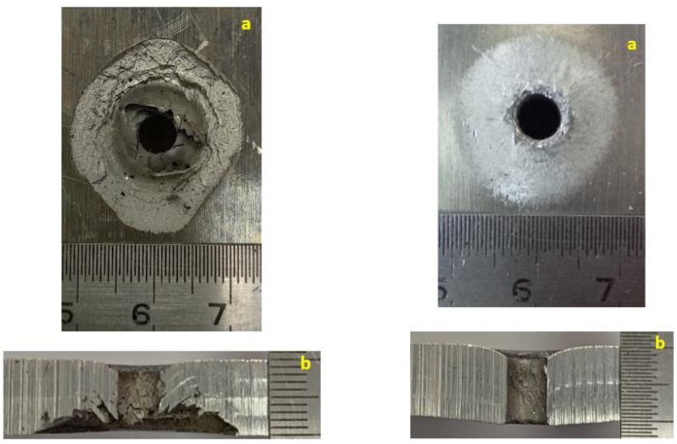

A B

**Figure 4: Aluminium plate exit hole images from target plate (A) A1 and (B) A2 plate configuration showing the (a) plate surface and (b) plate section.**

## 5. 7.62 x 51 mm APWC simulations

On completion of the experimental testing, it was clear that the modelled 7.62 APM2 bullet penetration performance at 930 m/s impact velocity is not similar to the 7.62 x 51 mm APWC bullet at the same impact velocity. Further simulations were conducted to determine whether numerical modelling could be used to predict the experimental results for the 7.62 x 51 mm APWC bullet. The same plate material properties shown in Tables A1, A2 and A3 were used, however the bullet needed to be re-modelled. A 7.62 x 51 mm bullet was weighed and sectioned and the actual measured geometry of the bullet was used, as far as possible, to create the new bullet model, see Figure 5. As with the 7.62 APM2 model, a mesh size of 0.4 mm was used for the projectile and plates and, as far as possible, only 8 node hexahedral elements were used. The JC material properties used for the WC projectile were taken from [23] and are shown in

Table , noting that the density was reduced slightly to match the measured mass of the projectile. A standard Ansys Explicit Dynamics material model was used for the aluminium sabot. As before, rotational velocity of the bullet was omitted.

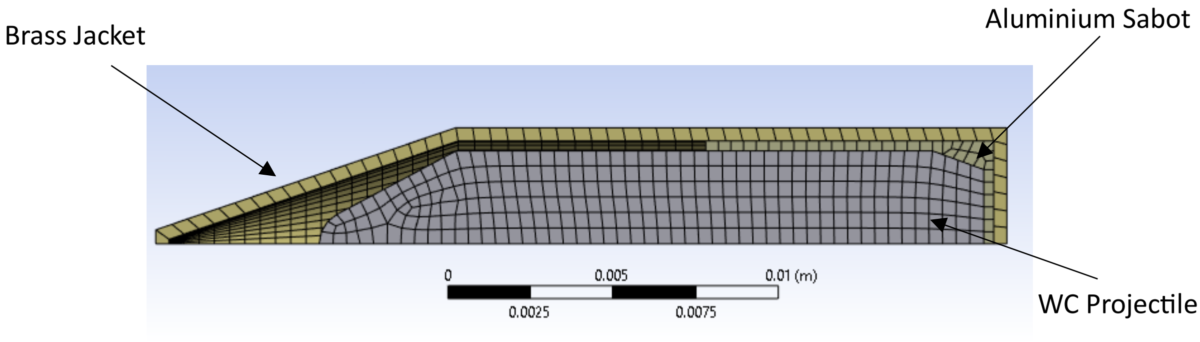


**Figure 5: Meshed quarter symmetry model of 7.62 x 51 mm bullet**

Simulations were run on each plate configurations listed in Table , at different impact velocities to enable the determination of the $v_{bl}$ using the Recht-Ipson formulation [19]. Once the Recht-Ipson parameters had been determined using the Matlab® Curve Fitting Toolbox [24], these parameters were used to estimate the $v_{bl}$ of the designed plate configurations using the actual impact velocities. The results of this approach are shown in

Figure **6** for the A1, A2 and A3 and B4 plate configurations. The difference between the simulated $v_{bl}$ and estimated experimental $v_{bl}$ values for these plate configurations were 14.4%, 5%, 8% and 76.9% respectively. A summary of the Richt-Ipson curves for the test and experimental results for all the plate configurations tested are shown in Table . For plates A2 and similarly for A3, the simulations emulated the more ductile deformation and failure the test plates underwent, whereas for plate A1, the simulation was unable to capture the brittle nature of the plate exit failure, as shown in Figure 7 and Figure 8.

**Table 3: Summary of simulated and estimated $v_{bl}$ values based on 7.62 x 51 mm APWC bullet impact simulations.**

| Code | Simulated $v_{bl}$ | Estimated $v_{bl}$ | % Difference |
|---|---|---|---|
| A1 | 835 | 730 | 14.4% |
| A2 | 800 | 760 | 5.3% |
| A3 | 810 | 750 | 8.0% |
| B1 | 830 | 650 | 27.7% |

| | | | |
|---|---|---|---|
| B2 | 800 | 618 | 29.4% |
| B3 | 1048 | 620 | 69.0% |
| B4 | 920 | 630 | 76.9% |
| C1 | 750 | 690 | 8.7% |

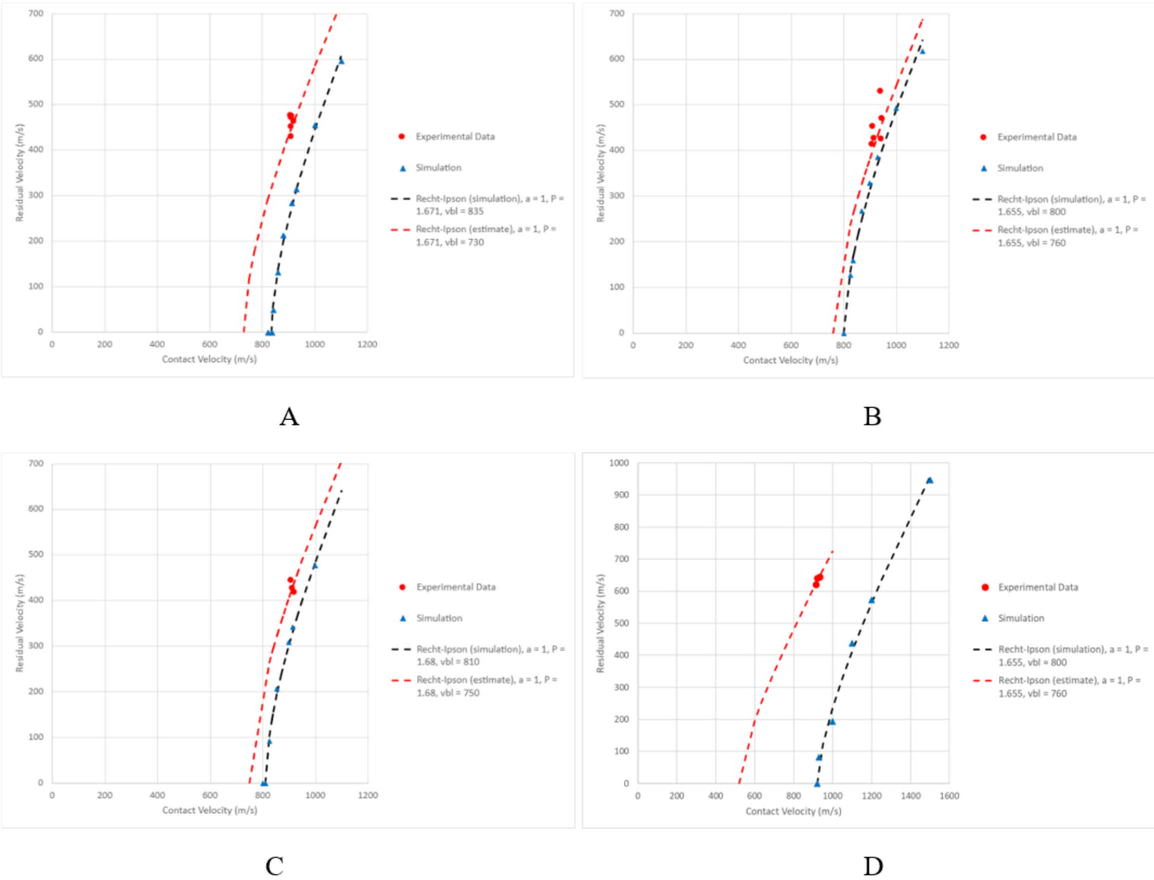


**Figure 6: Richt-Ipson plots of the simulations for plates (A) A1, (B) A2, (C) A3 and (D) B1 showing the simulation data, the fitted Recht-Ipson model as well as the experimental data and estimated $v_{bl}$ of the plate configuration.**


**Figure 7: Comparison of plate damage and deformation evident on sectioned plate (A2) versus simulation.**

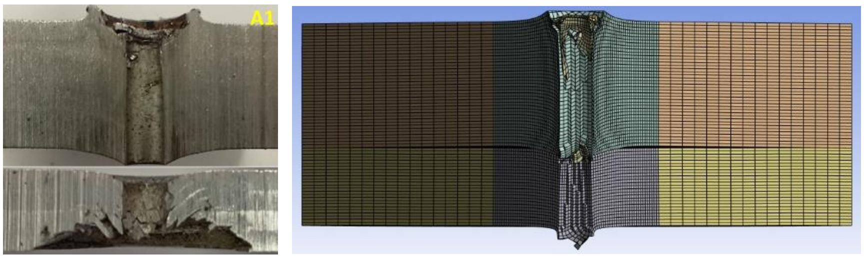

**Figure 8: Comparison of plate damage and deformation evident on sectioned plate (A1) versus simulation.**

## 6. Discussion

It is evident from the comparison of the literature, experimental and simulated results, presented as Richt-Ipson plots shown in Figure 6

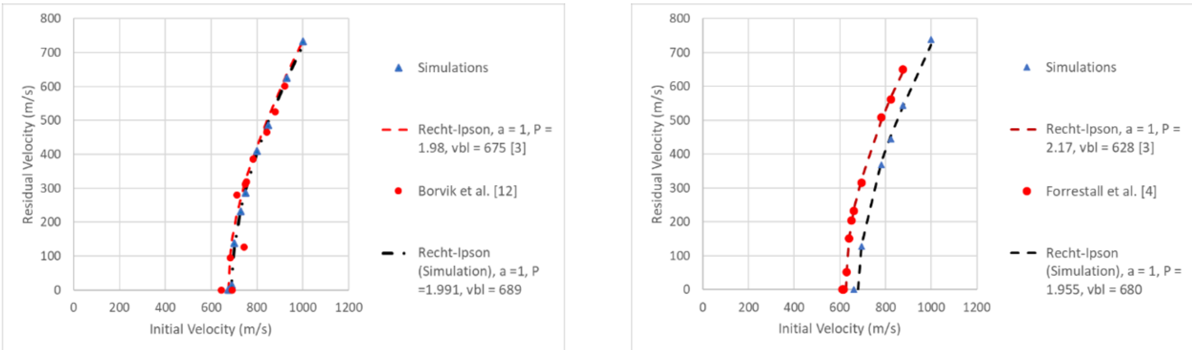


A B

, that the computational models for the Weldox 700E plate were significantly more accurate than those for the Al7075 T651. This is largely attributed to the use of literature data for the JC constitutive material properties as well as the JC failure model for Al7075 T651 that were not the same as the experimental results reported in [24]. There is also a significant question about the suitability of the JC failure model for brittle materials, particularly as it is more commonly used for ductile materials [25]. This is particularly relevant for the Al7075 T651 plate which may be significantly more brittle than the Weldox 700E plate. The results also raise the issue of whether the computational models accurately represent tensile failures at the free surfaces under impact loading. The accuracy of these models may also be improved if a failure model were used on the projectile material. Here again, when efforts were made to use the JC failure criterion on the WC projectile, the simulations generally ended with the projectile squashing into the target rather than penetrating it which once again brings into question the suitably of this failure model for these types of hard brittle materials.

The simulations of the 7.62 APM2 bullet impacting the designed plate configurations were consistent with the results shown in [5, 9] as the majority of the plate configurations stopped the projectile at 930 m/s with little or no penetration. The question over whether a double plate is better than a triple plate is still open for further investigation as the experimental results shown in this paper indicate that it largely depends on the materials used, the specific layering sequence and the failure mechanisms that occur in the individual plates. In this regard, these findings are consistent with the literature [23–25]. Evidently further research is required to fully understand how the failure mechanism of a plate changes depending on its position in the overall plate configuration and how this would affect the protection offered by different plate configurations.

What is evident by comparison of the simulation results for the 7.62 APM2 and 7.62 x 51 mm APWC is that the WC bullet offers a significantly greater penetration threat than its APM2 counterpart. This can be seen on the APM2 simulations that showed that at 930 m/s the plate configurations would be affective in stopping the bullet whereas, for the WC simulations and experimental results, at 930 m/s, all the plate configurations were easily penetrated.

Comparison of the 7.62 x 51 mm APWC simulations with the experimental results showed that all the simulations significantly underestimated the protection offered by the designed plate configurations. This is largely attributed to the material and failure models used in the computational model for the plate materials as well as the WC projectile. Specifically for the plates, it is evident that the failure behaviour of the aluminium plate changes depending on where in the plate configuration it is placed and, as has been shown, this behaviour has not been captured by the material and failure models used in the simulations.

With regard to the WC projectile, as has been reported in the literature, measuring the high strain rate properties and characterising the WC projectile materials, and then creating a verified material and failure model that captures its behaviour adequately, is an area of ongoing research and requires more investigation [23,25,26].

The simulation results for the metal-metal layered plates were useful for design purposes and can be used for future plate configuration developments as, particularly for the triple layered plates, the difference between the experimental and simulated results is acceptable. However, the plate configurations used in this work were ineffective at stopping the WC bullet. The results bring into question whether structural steel pates should be used on the impact face of ballistic protection and the suitability of Aluminium for this type of bullet. Similarly, using Dyneema and Kevlar panels in these configurations proved particularly unsuitable for ballistic protection against this type of bullet. In addition, it is evident from the simulation results for the Dyneema and Kevlar plates that the material model used in this work for these materials were not suitable.

## 7. Conclusion

This work has gone a long way to improving our understanding as to how, metal plates respond to bullet impact and provide ballistic protection. The use of computational simulations is clearly a viable option for future plate designs by providing protection improvement trends with multilayer panels, however, it is evident that the material and failure models need to be improved, and that, ideally, the properties of the bullets and the plate models should be experimentally extracted.

Based on this initial computational and test work it is believed that multi-layered plates can be used to reduce the areal density of protection plate configurations, however, it is questionable as to whether structural materials will be suitable, which will have a significant cost implication, especially when trying to stop the WC bullet. As ever, the challenge remains to reduce the weight and cost of the plates, whilst still meeting the required protection level.

## Nomenclature

| | |
|---|---|
| $\varepsilon$ | equivalent plastic strain |
| $\varepsilon^{f}$ | fracture strain |
| $\dot{\varepsilon}^{*}$ | dimensionless plastic strain at a specific strain rate |
| $\dot{\varepsilon}_0$ | strain rate |
| $\sigma$ | von Mises flow stress |
| $\sigma^{*}$ | dimensionless pressure-stress ratio |
| a | constant |
| $A$ | yield stress |
| $B$ | strain hardening parameter |
| $C$ | material constant |
| $D_1$ - $D_5$ | material constants |
| $P$ | fitting constant. |
| $m$ | material constant |

$n$ strain hardening parameter

$T^*$ homologous temperature

$v_{bl}$ ballistic limit

$V_r$ residual velocity

$V_i$ impact velocity

## Abbreviations

Al Aluminium

JC Johnson-Cook

WC Tungsten Carbide

## References


[1] K. Senthil and M. A. Iqbal, "Prediction of superior target layer configuration of armour steel, mild steel and aluminium 7075-T651 alloy against 7.62 AP projectile," *Structures*, vol. 29, pp. 2106–2119, Feb. 2021.

[2] N. A. Rahman, S. Abdullah, W. F. H. Zamri, M. F. Abdullah, M. Z. Omar, and Z. Sajuri, "Ballistic Limit of High-Strength Steel and Al7075-T6 Multi-Layered Plates Under 7.62-mm Armour Piercing Projectile Impact," *Latin American Journal of Solids and Structures*, vol. 13, no. 9, pp. 1658–1676, Sep. 2016.

[3] E. A. Flores-Johnson, M. Saleh, and L. Edwards, "Ballistic performance of multi-layered metallic plates impacted by a 7.62-mm APM2 projectile," *International Journal of Impact Engineering*, vol. 38, no. 12, pp. 1022–1032, Dec. 2011.

[4] M. J. Forrestal, T. Børvik, and T. L. Warren, "Perforation of 7075-T651 Aluminum Armor Plates with 7.62 mm APM2 Bullets," *Experimental Mechanics*, vol. 50, p. 1245, 2010.

[5] Z. Wei, D. Yunfei, C. Z. Sheng, and W. Gang, "Experimental investigation on the ballistic performance of monolithic and layered metal plates subjected to impact by blunt rigid projectiles," *International Journal of Impact Engineering*, vol. 49, pp. 115–129, Nov. 2012.

[6] S. Dey, T. Børvik, X. Teng, T. Wierzbicki, and O. S. Hopperstad, "On the ballistic resistance of double-layered steel plates: An experimental and numerical investigation," *International Journal of Solids and Structures*, vol. 44, no. 20, pp. 6701–6723, Oct. 2007.

[7] N. K. Gupta, M. A. Iqbal, and G. S. Sekhon, "Effect of projectile nose shape, impact velocity and target thickness on the deformation behavior of layered plates," *Int. J. Impact Eng.*, vol. 35, no. 1, pp. 37–60, Jan. 2008.

[8] J. A. Zukas and D. R. Scheffer, "Impact effects in multilayered plates," *International Journal of Solid Structures*, vol. 38, pp. 3321–3328, 2001.

[9] X. Teng, T. Wierzbicki, and M. Huang, "Ballistic resistance of double-layered armor plates," *International Journal of Impact Engineering*, vol. 35, no. 8, pp. 870–884, Aug. 2008.

[10] J. Radin and W. Goldsmith, "Normal Projectile Penetration and Perforation of Layered Targets," *International Journal of Impact Engineering*, vol. 7, no. 2, pp. 229–259, 1988.
[11] X. Teng, S. Dey, T. Børvik, and T. Wierzbicki, "Protection performance of double-layered metal shields against projectile impact," *Journal of Mechanics of Materials and Structures*, vol. 2, no. 7, pp. 1309–1329, Sep. 2007.
[12] T. Børvik, S. Dey, and A. H. Clausen, "Perforation resistance of five different high-strength steel plates subjected to small-arms projectiles," *International Journal of Impact Engineering*, vol. 36, no. 7, pp. 948–964, Jul. 2009.
[13] Nato Standardization Agency, "Procedures for evaluating the protection level of armoured vehicles-kinetic energy and artillery threat," NATO AEP-55-vol 1 (Ed2), 2011.
[14] Nato Standardization Agency, "Stanag 4569 (Edition 2): Protection Levels for Occupants of Armoured Vehicles," AC/225-D(2011)0012 (PFP), 2011.
[15] G. R. Johnson and W. H. Cook, "A constitutive model and data for metals subjected to large strains, high strain rates, and high temperatures," presented at the Proceedings 7th International Symposium on Ballistics, The Hague, 1983.
[16] G. R. Johnson and W. H. Cook, "Fracture characteristics of three metals subjected to various strains, strain rates, temperatures and pressures," *Eng. Fract. Mech.*, vol. 21, no. 1, pp. 31–48, Jan. 1985.
[17] S. Dey, T. Børvik, O. S. Hopperstad, and M. Langseth, "On the influence of fracture criterion in projectile impact of steel plates," *Computational Materials Science*, vol. 38, no. 1, pp. 176–191, Nov. 2006.
[18] K. Senthil, M. A. Iqbal, P. S. Chandel, and N. K. Gupta, "Study of the constitutive behavior of 7075-T651 aluminum alloy," *International Journal of Impact Engineering*, vol. 108, pp. 171–190, Oct. 2017.
[19] R. F. Recht and T. W. Ipson, "Ballistic Perforation Dynamics," *Journal of Applied Mechanics*, vol. 30, no. 3, pp. 384–390, Sep. 1963.
[20] T. J. Holmquist, G. R. Johnson, and W. A. Gooch, "Modeling the 14.5 mm BS41 projectile for ballistic impact computations," in *Projectile Impact*, WIT Press, 2014, pp. 73–86.
[21] The MathWorks Inc., *Curve Fitting Toolbox: 3.5.13 (R2021a)*. Natick, Massachusetts, United States: The MathWorks Inc., 2023.
[22] J. F. Moxnes, J. A. Teland, S. Skriudalen, S. M. Bergsrud, L. Sundem-Eriksen, and H. Fykse, "Development of material models for semi-brittle materials like tungsten carbide," Norwegian Defence Research Establishment (FFI), FFI-rapport 2010/02225, 2010.
[23] C. Francart, "Mechanical characterization and modeling of the stress flow of a cemented tungsten carbide over wide ranges of temperatures and strain rates," *hal-04165509*, 2023.
[24] D.-N. Zhang, Q.-Q. Shangguan, C.-J. Xie, and F. Liu, "A modified Johnson–Cook model of dynamic tensile behaviors for 7075-T6 aluminum alloy," *Journal of Alloys and Compounds*, vol. 619, pp. 186–194, Jan. 2015.
[25] L. M. Bresciani, A. Manes, A. Ruggiero, G. Iannitti, and M. Giglio, "Experimental tests and numerical modelling of ballistic impacts against Kevlar 29 plain-woven fabrics with an epoxy matrix: Macro-homogeneous and Meso-heterogeneous approaches," *Composites Part B*, vol. 88, pp. 114–130, Mar. 2016.
[26] M. K. Hazzard, R. S. Trask, U. Heisserer, M. Van Der Kamp, and S. R. Hallett, "Finite element modelling of Dyneema® composites: From quasi-static rates to ballistic impact," *Composites. Part A, Applied Science and Manufacturing*, vol. 115, pp. 31–45, Dec. 2018.

# Appendix A: Material Properties used in simulations.

**Table A1: Johnson Cook material parameters used for validating the 7.62 APM2 model and the target plate design.**

| Property | Material | | | | | |
|---|---|---|---|---|---|---|
| | **Weldox / Strenx 700E** [12] | **Aluminium 7075 T651** [18] | **Aluminium 7075 T6** [20] | **Brass Jacket** [3] | **Lead Tip** [3] | **Steel Projectile** [3] |
| Density (kg/m$^3$) | 7850 | 2700 | 2700 | 8520 | 10600 | 7850 |
| Modulus (GPa) | 210 | 64 | 64 | 115 | 1 | 210 |
| Poisson's Ratio | 0.3 | 0.31 | 0.31 | 0.31 | 0.42 | 0.33 |
| A (MPa) | 819 | 448.45 | 448.45 | 206 | 24 | 1200 |
| B (MPa) | 308 | 475.808 | 475.808 | 505 | 3.00E+02 | 50000 |
| n | 0.64 | 0.3948 | 0.3948 | 0.42 | 1.00E+00 | 1 |
| Reference Strain Rate (s$^{-1}$) | 0.0005 | 0.0001 | 0.0001 | 0.01 | 0.0005 | 0.0005 |
| C | 0.0098 | 0.0012 | 0.0012 | 0.0005 | 0.1 | 0.1 |
| Tm (Degree C) | 1527 | 620 | 620 | 916 | 487 | 1527 |
| m | 1 | 1.29 | 1.29 | 1.68 | 1 | 1 |

**Table A2: Johnson Cook damage model parameters used for validating the 7.62 APM2 model and the target plate design.**

| Constant | Material | | |
|---|---|---|---|
| | **Strenx 700E** [17] | **Aluminium 7075 T651** [18] | **Aluminium 7075 T6** [20] |
| D1 | 0.361 | -0.428 | 0.3714 |
| D2 | 4.768 | 0.7566 | -0.1233 |

| | | | |
|---|---|---|---|
| D3 | -5.107 | -3.4078 | -1.9354 |
| D4 | -0.0013 | -0.003 | 0.0101 |
| D5 | 1.333 | 24.93 | 0 |

**Table A3: Orthotropic material parameters for Kevlar® 29 and Dyneema® HB26**

| Property | Kevlar® 29 [21] | Dyneema® HB26 [22] |
|---|---|---|
| Modulus, X (MPA) | 18500 | 34257 |
| Modulus, Y (MPA) | 18500 | 34257 |
| Modulus, Z (MPA) | 6000 | 3260 |
| Poisson's Ratio, XY | 0.25 | 0 |
| Poisson's Ratio, YZ | 0.33 | 0.013 |
| Poisson's Ratio, XZ | 0.33 | 0.013 |
| Shear Modulus, XY (MPA) | 770 | 173.8 |
| Shear Modulus, YZ (MPA) | 5430 | 547.8 |
| Shear Modulus, XZ (MPA) | 5430 | 547.8 |

**Table A4: JC parameters of WC projectile taken from [23].**

| Property | WC projectile |
|---|---|
| Density ($kg/m^3$) | 13805 |
| Modulus (GPa) | 620 |
| Poisson's Ratio | 0.215 |
| A (MPa) | 3000 |
| B (MPa) | 89000 |
| n | 0.65 |
| Reference Strain Rate ($s^{-1}$) | 1 |
| C | 0 |
| Tm (Degree C) | 1527 |
| m | 1 |